ARCHIVES OF MECHANICS
Arch. Mech. **73** (3), 253–266, 2021, DOI: 10.24423/aom.3765

# Ponding on an inflated tube and the membrane trough

C. Y. WANG

*Departments of Mathematics and Mechanical Engineering, Michigan State University, East Lansing, MI 48824, U.S.A., e-mail: cywang@mth.msu.edu*

The ponding on an inflated membrane tube is studied. Membrane tubes have the advantage of zero leakage and ease of transportation and set-up. A novel related problem is the membrane trough which can be used to contain water and does not need anchoring. These problems depend on two non-dimensional parameters which characterize membrane tension and pressure. Perturbation solutions to second order are found for shallow ponding, and compare well with those of exact numerical integration. Tables for the pertinent parameters are constructed and cross section geometries are found. This research illustrates the interaction of membrane structure, pressure load, and hydrostatics.

**Key words:** ponding, membrane, inflated, tube, trough.



## 1. Introduction

Inflated membrane structures have been used as enclosures for shelters, warehouses, and sports arenas [1,2]. Inflated membrane tubes are also used as storage for gasses, floating devices, and flood control [3–5].

Inflated membrane cylinders can be subjected to ponding, i.e. accumulation of rain water, sand, ice, or snow on the top. Ponding may lead to collapse of the membrane structure. Using a linear approximation, Malcolm and Glockner [6] considered the ponding on an inflated circular arc membrane cylinder with an added center load. Extension to the asymmetric loading case was done by Lukasiewicz and Glockner [7]. Maaskant and Roorda [8] used elliptic functions to study the large deformations due to ponding and established stability criteria.

All previous literature considered the inflated circular arc membrane cylinder anchored at longitudinal edges. The aim of the present paper is as follows. Firstly, we study the nonlinear deformations due to ponding on a complete membrane tube. This enclosed geometry is especially important for the storage of gasses. Secondly, we propose utilizing ponding as a new type of water containment. Applications may include temporary recreational pools, livestock water troughs and open channels for water transport. The two problems are related.

We shall assume the membrane tube is long (two-dimensional), inextensible and its own weight is negligible. The ponded water, or other material, exerts hydrostatic pressure on the membrane.

## 2. Formulation

Figure 1(a) shows the cross section of a ponding on an inflated membrane tube. Let the pressure inside the tube be $p_0$ and the ambient pressure be $p_a$. Let the total peripheral length of the tube be $L$ and the height of the impounded fluid be $H$. The origin of the Cartesian axes $(x', y')$ is at the bottom of the ponding. Let $s'$ be the arc length from the origin and $\theta$ be the local angle of inclination. The wetted section is from 0 to $s^{*\prime}$ where the membrane is subjected to hydrostatic pressure. From $s^{*\prime}$ to $\hat{s}'$ the membrane is circular due to the constant pressure difference. The membrane is in contact with ground after $\hat{s}'$. The distance from the origin to the ground is $d'$. Figure 1(b) shows the right half, where all lengths have been normalized by $H$ and the primes are dropped. When $d$ is zero, we obtain the right end of a membrane trough shown in Fig. 1(c).

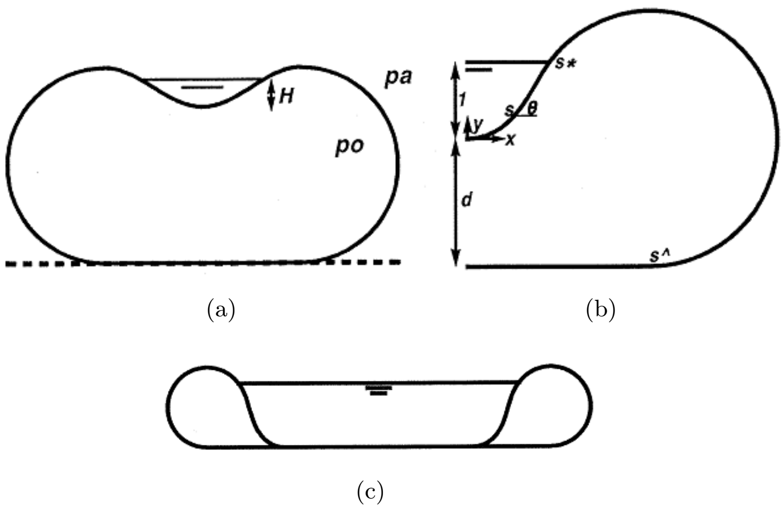


FIG. 1. (a) Membrane tube under ponding. (b) Normalized coordinates. (c) A membrane trough.

For the wetted segment the governing equation is

$$-T\frac{d\theta}{ds'} = p_0 - [p_a + \rho g(H - y')]. \tag{2.1}$$

Here $T$ is the tension of the membrane, $\rho$ is the density of water, and $g$ is the gravitation acceleration. For the segment exposed to ambient air the equation is

$$-T\frac{d\theta}{ds'} = p_0 - p_a. \tag{2.2}$$

The coordinates are kinematically related by

$$\frac{dx'}{ds'} = \cos\theta, \qquad \frac{dy'}{ds'} = \sin\theta. \tag{2.3}$$

In the normalized variables, Eq. (2.1) becomes

$$\alpha\frac{d\theta}{ds} = 1 - \beta - y, \tag{2.4}$$

where

$$\alpha = \frac{T}{\rho g H^2}, \qquad \beta = \frac{p_0 - p_a}{\rho g H} \tag{2.5}$$

are important positive non-dimensional parameters representing membrane tension and pressure difference respectively. Equations (2.3) become

$$\frac{dx}{ds} = \cos\theta, \qquad \frac{dy}{ds} = \sin\theta. \tag{2.6}$$

The boundary conditions are that

$$\theta(0) = 0, \quad x(0) = 0, \quad y(0) = 0. \tag{2.7}$$

At the transition point $s = s^*$, $y(s^*) = 1$, $\theta$ is continuous, and at the next touching point $s = \hat{s}$,

$$y(\hat{s}) = -d, \qquad \theta(\hat{s}) = -\pi. \tag{2.8}$$

The tension parameter $\alpha$ is unknown. The problem is formidable as it is.

## 3. Some analytic observations

For the wetted part, Eq. (2.4) can be written as

$$\alpha\frac{d\theta}{dy}\sin\theta = 1 - \beta - y \tag{3.1}$$

which after integration once and using Eqs. (2.7a, c)

$$\alpha(1 - \cos\theta) = (1 - \beta)y - y^2/2. \tag{3.2}$$

At transition, Eq. (3.2) is

$$\alpha(1 - \cos\theta^*) = \frac{1}{2} - \beta, \tag{3.3}$$

where $\theta^* = \theta(s^*)$. If water is filled to the brim, $\theta^* = 0$ and Eq. (3.3) shows $\beta = 0.5$ regardless of $\alpha$.

For the exposed segment Eq. (2.2) gives

$$\frac{d\theta}{ds} = -\frac{\beta}{\alpha}. \tag{3.4}$$

Integration gives

$$\theta = -\frac{\beta}{\alpha}(s - s^*) + \theta^*. \tag{3.5}$$

Equation (2.6b) yields

$$\frac{dy}{ds} = \sin\left[-\frac{\beta}{\alpha}(s - s^*) + \theta^*\right]. \tag{3.6}$$

Integrating and using $y(s^*) = 1$ result in

$$y = \frac{\alpha}{\beta}\left\{\cos\left[-\frac{\beta}{\alpha}(s - s^*) + \theta^*\right] - \cos\theta^*\right\} + 1. \tag{3.7}$$

But Eqs. (2.8b) and (3.5) give

$$-\frac{\beta}{\alpha}(\hat{s} - s^*) + \theta^* = -\pi. \tag{3.8}$$

Thus at $s = \hat{s}$ Eqs. (2.8a), (3.7) and (3.8) give

$$\frac{\alpha}{\beta}(-1 - \cos\theta^*) + 1 = \hat{y} \leq 0. \tag{3.9}$$

Solving Eqs. (3.3) and (3.9) gives the distance

$$d = -\hat{y} = \frac{1}{2\beta}(4\alpha - 1) \tag{3.10}$$

also

$$\cos\theta^* = 1 + \frac{1}{\alpha}\left(\beta - \frac{1}{2}\right). \tag{3.11}$$

Notice that cosine is less than one, thus $0 < \beta \leq 0.5$. Using Eqs. (3.6) and (3.7) the maximum height is

$$y_m = \frac{\alpha}{\beta}(1 - \cos\theta^*) + 1 = \frac{1}{2\beta}, \tag{3.12}$$

occurring at

$$s = s^* + \frac{\alpha\theta^*}{\beta}, \tag{3.13}$$

where $\theta^*$ is from Eq. (3.11). The total height of the membrane tube is

$$y_m + d = \frac{2\alpha}{\beta} \tag{3.14}$$

is the volume of water per depth impounded is of interest. The half volume, normalized by $H^2$ is

$$v = \int_0^{y^*} x\,dy = \int_0^{s^*} x \sin\theta\,ds. \tag{3.15}$$

Using Eq. (3.5), integrate Eq. (2.6a) to obtain

$$x = x^* - \frac{\alpha}{\beta}\left\{\sin\left[-\frac{\beta}{\alpha}(s - s^*) + \theta^*\right] - \sin\theta^*\right\}. \tag{3.16}$$

Equations (3.8) and (3.16) yield

$$\hat{x} = x^* + \frac{\alpha}{\beta}\sin\theta^* = a. \tag{3.17}$$

The perimeter length $l$ of the right half is

$$l = a + \hat{s} = x^* + s^* + \frac{\alpha}{\beta}(\pi + \theta^* + \sin\theta^*). \tag{3.18}$$

In order to normalize by the total perimeter length $L = 2lH$ instead of the height of the fluid $H$, divide all normalized lengths and $\beta$ by $2l$, and $\alpha$ by $4l^2$.

For the wetted segment, differentiate Eq. (2.4) to eliminate $\beta$

$$\frac{d^2\theta}{ds^2} = -\frac{1}{\alpha}\sin\theta. \tag{3.19}$$

Multiply by $d\theta/ds$ to get the first integral

$$\frac{1}{2}\left(\frac{d\theta}{ds}\right)^2 = \frac{1}{\alpha}\cos\theta + c, \tag{3.20}$$

where from Eqs. (2.4), (2.7a), (2.7c)

$$c = \frac{1}{2\alpha^2}(1-\beta)^2 - \frac{1}{\alpha}. \tag{3.21}$$

Taking the square root of Eq. (3.20) and integrating, one can express $s$ in terms of elliptic functions in $\theta$. This method is very tedious, and numerical evaluations are still needed to apply the boundary conditions. In a later section we use a simpler initial value integration.

## 4. Perturbation solution for shallow ponding

If tension is large, the amount of possible ponding would be small. We expect a shallow layer on top of the membrane tube. Since the $y$ coordinate was normalized to order unity, the $s$ and $x$ coordinates would be large. Define a small number $\varepsilon$

$$\varepsilon = \frac{1}{\sqrt{\alpha}} \ll 1. \tag{4.1}$$

An order of magnitude analysis suggests the expansions

$$s = \frac{t}{\varepsilon}, \quad \theta = \varepsilon\theta_0(t) + \varepsilon^3\theta_1(t) + O(\varepsilon^5), \tag{4.2}$$

$$y = y_0(t) + \varepsilon^2 y_1(t) + O(\varepsilon^4), \quad x = \frac{1}{\varepsilon}x_0(t) + \varepsilon x_1(t) + O(\varepsilon^3), \tag{4.3}$$

where $t$ is of order unity, and all functions of $t$ are of order unity. Substitution into Eq. (3.19) and comparing like powers of $\varepsilon$ yield

$$\frac{d^2\theta_0}{dt^2} = -\theta_0, \qquad \frac{d^2\theta_1}{dt^2} = -\left(\theta_1 - \frac{1}{6}\theta_0^3\right). \tag{4.4}$$

Since $\theta_0(0) = \theta_1(0) = 0$, the solutions to Eqs. (4.4) are

$$\theta_0 = c_0 \sin t, \tag{4.5}$$

$$\theta_1 = \frac{c_0^3}{192}[\sin(3t) - 12t\cos t] + c_1 \sin t. \tag{4.6}$$

Here $c_0$, $c_1$ are constants to be determined. Expansion of Eq. (2.6b) gives

$$\frac{dy_0}{dt} = \theta_0, \qquad \frac{dy_1}{dt} = \theta_1 - \frac{1}{6}\theta_0^3. \tag{4.7}$$

The solution to Eq. (4.7a) which is zero at the origin is

$$y_0 = c_0(1 - \cos t). \tag{4.8}$$

Due to normalization, the boundary conditions at the transition point $t^*$ are

$$y_0(t^*) = 1, \quad y_1(t^*) = 0. \tag{4.9}$$

Equations (4.8) and (4.9a) give

$$c_0 = \frac{1}{1 - \cos t^*}. \tag{4.10}$$

On the other hand, the leading order of Eq. (2.4) is

$$\frac{d\theta_0}{dt} = 1 - \beta - y_0. \tag{4.11}$$

Substitution of Eqs. (4.5) and (4.8) yields

$$\beta = 1 - c_0 = \frac{-\cos t^*}{1 - \cos t^*}. \tag{4.12}$$

Or given $\beta$, the location $t^*$ can be found independent of tension $\alpha$

$$t^* = \cos^{-1}\left(\frac{\beta}{\beta - 1}\right). \tag{4.13}$$

Since $0 < \beta \le 0.5$, thus $0.5\pi < t^* \le \pi$. After some work, the solution to Eq. (4.7b) is

$$y_1 = \frac{1}{64}\{c_0^3[1 - \cos(3t)] - 4c_0^3 t \sin t + 4(1 - \cos t)(16c_1 - c_0^3)\}. \tag{4.14}$$

Equation (4.9b) then gives

$$c_1 = \frac{3 - 4\cos t^* + \cos(3t^*) + 4t^* \sin t^*}{64(1 - \cos t^*)^4}. \tag{4.15}$$

Expansion of Eq. (2.6a) gives

$$\frac{dx_0}{dt} = 1, \qquad \frac{dx_1}{dt} = -\frac{1}{2}\theta_0^2. \tag{4.16}$$

The solution with zero initial condition is

$$x_0 = t, \qquad x_1 = \frac{c_0^2}{8}[\sin(2t) - 2t]. \tag{4.17}$$

As for the volume, Eq. (3.15) is perturbed by substituting Eqs. (4.2) and (4.3b)

$$v = \frac{1}{\varepsilon} v_0(t^*) + \varepsilon v_1(t^*) + O(\varepsilon^3), \tag{4.18}$$

where

$$v_0 = \int_0^{t^*} x_0\theta_0 \, dt = c_0(\sin t^* - t^* \cos t^*), \tag{4.19}$$

$$\begin{aligned} v_1 &= \int_0^{t^*} \left[x_1\theta_0 + x_0\left(\theta_1 - \frac{1}{6}\theta_0^3\right)\right] dt \\ &= \frac{1}{64}[16(c_0^3 - 4c_1)t^* \cos t^* - c_0^3 t^* \cos(3t^*) \\ &\qquad + 64c_1 \sin t^* - 4c_0^3(3 + {t^*}^2) \sin t^* - c_0^3 \sin(3t^*)]. \end{aligned} \tag{4.20}$$

Given $\beta$ and large $\alpha$, Eq. (4.13) gives $t^*$ and

$$s^* = \sqrt{\alpha}t^*, \qquad y^* = 1, \tag{4.21}$$

$$\theta^* = \alpha^{-1/2}\theta_0(t^*) + \alpha^{-3/2}\theta_1(t^*) + O(\alpha^{-5/2}), \tag{4.22}$$

$$x^* = \alpha^{1/2}x_0(t^*) + \alpha^{-1/2}x_1(t^*) + O(\alpha^{-3/2}), \tag{4.23}$$

$$v = \alpha^{1/2}v_0(t^*) + \alpha^{-1/2}v_1(t^*) + O(\alpha^{-3/2}). \tag{4.24}$$

Then from Eqs. (3.8), (3.9) and (3.17)

$$\hat{s} = s^* + (\theta^* + \pi)\frac{\alpha}{\beta} = \alpha\frac{\pi}{\beta} + \alpha^{1/2}\left(t^* + \frac{\theta_0^*}{\beta}\right) + O(\alpha^{-1/2}), \tag{4.25}$$

$$\hat{x} = \alpha^{1/2}\left[x_0(t^*) + \frac{1}{\beta}\theta_0(t^*)\right] + \alpha^{-1/2}\left[x_1(t^*) + \frac{1}{\beta}\theta_1(t^*) - \frac{1}{6\beta}\theta_0^3(t^*)\right] + O(\alpha^{-3/2}), \tag{4.26}$$

$$\hat{y} = \frac{-1}{2\beta}(4\alpha - 1). \tag{4.27}$$

The half perimeter length is $l = \hat{s} + \hat{x}$. These perturbation results shall be compared with those of the exact numerical integration.

## 5. The membrane trough

Inflatable membrane cylinders have been used as temporary dams for water containment [9–11, 3]. Usually a membrane strip is anchored along the two longitudinal edges. In order to minimize leakage from the strip, a membrane tube can be used, but the tube still needs to be anchored to prevent lateral movement. Kim *et al.* [12] attached an apron on the wetted side, using hydrostatic pressure as the anchor. Expanding on this idea, we propose a membrane trough which has the advantage of zero leakage and complete anchoring.

This membrane trough is very related to the ponding problem in previous sections. When ponding is severe, the center part of the tube collapsed. This can be used as a membrane trough shown in Fig. 1(c). Only the right inflated section needs to be considered. Due to the arbitrary length of the collapsed section, the total perimeter length of the tube is now irrelevant.

We require the distance $d$ in Fig. 1(b) to be zero. From Eq. (3.10) the normalized tension is determined:

$$\alpha = \frac{1}{4}. \tag{5.1}$$

The maximum height of the trough is $\frac{1}{2\beta}$. The analyses are the same as before, except the perturbation results (for large $\alpha$ or shallow ponding) are not applicable.

## 6. Results and discussions

For any given $\alpha$ and $\beta$ Eqs. (2.4), (2.6) and (2.7) can be numerically integrated as an initial value problem by a Runge–Kutta algorithm. The integration stops when $y = 1$ where we note $s^*$, $\theta^*$, $x^*$. The solution to the exposed circular segment is then Eq. (3.5), and the circular arc ends at $\hat{s}$ from Eq. (3.8). The distance $d$ is found from Eq. (3.10) and the half perimeter length from Eq. (3.18).

The reason why the ponding height $H$ is used as length scale instead of the tube perimeter length $L$ is as follows. The length $H$ quantifies the wetted region, where perturbation and numerical computations are needed. Also, for the membrane trough, only the height $H$ matters.

Table 1 shows our results. Our perturbation results compare well with those of numerical integration for large $\alpha$, and sometime even valid down to $\alpha = 0.5$.

**Table 1. Essential design parameters. Perturbation results are in parentheses. Only values that differ with numerical results within 5% are shown.**

| $\beta = 0.5$ | | | | | |
|---|---|---|---|---|---|
| $\alpha$ | 0.25 | 0.5 | 1 | 2 | 5 |
| $s^*$ | 1.686 | 2.296 (2.221) | 3.192 (3.142) | 4.478 (4.428) | 6.995 (7.025) |
| $\theta^*$ | 0 | 0 | 0 (0.0245) | 0 (0.0087) | 0 (0.0022) |
| $x^*$ | 1.249 | 2.004 (1.944) | 2.991 (2.945) | 4.338 (4.304) | 6.914 (6.937) |
| $v$ | 0.6246 | 1.002 (1.007) | 1.496 (1.497) | 2.169 (2.169) | 3.478 (3.479) |
| $\hat{x}$ | 1.249 | 2.004 (2.013) | 2.991 (2.994) | 4.338 (4.339) | 6.914 (6.959) |
| $\hat{y}$ | 0 | $-1$ | $-3$ | $-7$ | $-19$ |
| $\hat{s}$ | 3.257 | 5.438 (5.363) | 9.471 (9.425) | 17.05 (17.01) | 38.41 (38.44) |
| $l$ | 4.506 | 7.442 (7.376) | 12.47 (12.42) | 21.38 (21.35) | 45.33 (45.40) |

| $\beta = 0.4$ | | | | | |
|---|---|---|---|---|---|
| $\alpha$ | 0.25 | 0.5 | 1 | 2 | 5 |
| $s^*$ | 1.313 | 1.727 | 2.367 (2.301) | 3.299 (3.253) | 5.173 (5.144) |
| $\theta^*$ | 0.9273 | 0.6436 | 0.4510 | 0.3176 (0.3309) | 0.2003 (0.2037) |
| $x^*$ | 0.7141 | 1.342 | 2.106 (2.049) | 3.118 (3.075) | 5.059 (5.032) |
| $v$ | 0.4856 | 0.8366 (0.8071) | 1.496 (1.497) | 2.169 (2.169) | 3.019 (3.007) |
| $\hat{x}$ | 1.214 | 2.092 (2.155) | 3.195 (3.233) | 4.679 (4.704) | 7.547 (7.561) |
| $\hat{y}$ | 0 | $-1.25$ | $-3.75$ | $-8.75$ | $-23.75$ |
| $\hat{s}$ | 3.856 | 6.458 (6.344) | 11.35 (11.27) | 20.60 (20.54) | 46.95 (46.91) |
| $l$ | 5.070 | 8.550 (8.500) | 14.54 (14.51) | 25.27 (25.25) | 54.49 (54.48) |

**Table 1. [cont.]**

| $\beta = 0.3$ | | | | | |
|---|---|---|---|---|---|
| $\alpha$ | 0.25 | 0.5 | 1 | 2 | 5 |
| $s^*$ | 1.224 | 1.547 | 2.093 (2.014) | 2.902 (2.848) | 4.536 (4.503) |
| $\theta^*$ | 1.370 | 0.9273 | 0.6435 | 0.4510 (0.4691) | 0.2838 (0.2884) |
| $x^*$ | 0.4570 | 1.081 | 1.783 (1.720) | 2.688 (2.640) | 4.403 (4.371) |
| $v$ | 0.3820 | 0.7243 | 1.135 (1.103) | 1.678 (1.654) | 2.721 (2.705) |
| $\hat{x}$ | 1.274 | 2.415 | 3.783 (3.894) | 5.594 (5.668) | 9.020 (9.115) |
| $\hat{y}$ | 0 | −1.667 | −5 | −11.67 | −31.67 |
| $\hat{s}$ | 4.983 | 8.328 (8.151) | 14.71 (14.59) | 26.85 (26.77) | 61.63 (61.58) |
| $l$ | 6.257 | 10.74 (10.74) | 18.49 (18.491) | 32.45 (32.44) | 70.70 (70.69) |

| $\beta = 0.2$ | | | | | |
|---|---|---|---|---|---|
| $\alpha$ | 0.25 | 0.5 | 1 | 2 | 5 |
| $s^*$ | 1.204 | 1.436 | 1.915 (1.824) | 2.640 (2.579) | 4.115 (4.077) |
| $\theta^*$ | 1.772 | 1.159 | 0.7954 | 0.5548 (0.5779) | 0.3482 (0.3541) |
| $x^*$ | 0.2263 | 0.8915 | 1.561 (1.493) | 2.399 (2.345) | 3.965 (3.930) |
| $v$ | 0.2902 | 0.6365 | 1.026 (0.9878) | 1.533 (1.504) | 2.499 (2.480) |
| $\hat{x}$ | 1.448 | 3.183 | 5.132 | 7.666 (7.851) | 12.50 (12.61) |
| $\hat{y}$ | 0 | −2.5 | −7.5 | −17.5 | −47.5 |
| $\hat{s}$ | 7.347 | 12.19 (11.88) | 21.60 (21.40) | 39.60 (39.47) | 91.36 (91.28) |
| $l$ | 8.798 | 15.37 (15.50) | 26.73 (26.81) | 47.27 (47.32) | 103.9 (103.9) |

| $\beta = 0.1$ | | | | | |
|---|---|---|---|---|---|
| $\alpha$ | 0.25 | 0.5 | 1 | 2 | 5 |
| $s^*$ | 1.267 | 1.361 | 1.786 | 2.447 (2.379) | 3.803 (3.761) |
| $\theta^*$ | 2.214 | 1.370 | 0.9273 | 0.6435 (0.6719) | 0.4027 (0.4100) |
| $x^*$ | −0.0462 | 0.7360 | 1.389 (1.319) | 2.180 (2.122) | 3.638 (3.599) |
| $v$ | 0.1954 | 0.5634 | 0.9389 (0.8957) | 1.418 (1.385) | 2.324 (2.302) |
| $\hat{x}$ | 1.954 | 5.635 | 9.389 | 14.18 (14.72) | 23.23 (23.56) |
| $\hat{y}$ | 0 | −5 | −15 | −35 | −95 |
| $\hat{s}$ | 14.66 | 23.92 (23.22) | 42.47 (42.04) | 78.15 (77.86) | 181.0 (180.8) |
| $l$ | 16.61 | 29.55 (30.11) | 51.86 (52.23) | 92.33 (92.58) | 204.3 (204.4) |

As noted before, all lengths in the table have been normalized by the height of the ponding $H$. In order to normalize by the perimeter of a membrane tube, one needs to divide the length entries by $2l$, where $l$ is the half length of the perimeter, normalized by $H$. Similarly for the volume or the parameters $\alpha$ and $\beta$ all of which have been normalized with $H$. As for a membrane trough, the total perimeter is $2l + 2b$ where $b$ could be any length of the collapsed segment.

The parameter $\beta$ is the pressure difference normalized by $H$. Equation (3.11) shows $\beta = 0.5$ is the limit when water fully fills (to the brim) of the ponding.

Partially filled cases are possible when some water is added or removed, or when the pressure difference is decreased while the fluid volume (or mass) remains the same. Thus $0 < \beta/0.5 \leq 1$ is a measure of the fractional level of filling in the depression.

The parameter $\alpha$ represents tension normalized by $H^2$. For given filling level $\beta$, Eq. (3.12) shows $(4\alpha - 1)$ is proportional to $d$, or the distance to the ground normalized by the thickness of the ponding. For the membrane trough $\alpha = 1/4$ and for general membrane tubes $\alpha \geq 0.25$.

From the tables we see that when $\beta$ increases, $\theta^*$, $\hat{s}$, $l$ and $d = -\hat{y}$ decrease, $v$, $x^*$ increase, and $\hat{x}$, $s^*$ first decrease then increase. When $\alpha$ increases, all the listed parameters increase, except for $\theta^*$ which decreases.

As an example, consider a given membrane tube with the pressure difference maintained constant. The ponding is now gradually increased due to precipitation. Thus the dimensional half perimeter length $l'$ is fixed and $p_0 - p_a$ is fixed. Since the ponding height $H$ varies, it is eliminated from $l' = lH$ and Eq. (2.5b) to obtain

$$\frac{p_0 - p_a}{\rho g l'} = \frac{\beta}{l}. \tag{6.1}$$

Let's just say the left side of Eq. (6.1) is evaluated to be 0.01. For given $\beta$ or partial fill, the normalized half-length is $l = \beta/0.01$. From interpolation in Table 1 or from computation the following parameters in Table 2 are obtained for this particular case. Since in dimensional form $l' = lH$, $v' = vH^2$ we find

$$\frac{v'}{l'^2} = \frac{v}{l^2}. \tag{6.2}$$

The actual volume impounded is not $v$ but $v$' which is proportional to $\frac{v}{l^2}$ in Table 2. We see as $\beta$ is decreased, the actual volume increases. The $\beta = 0.1$ case is absent since the tube has partially collapsed and the tube becomes a membrane trough. Figure 2 shows the cross sections of the membrane tube as ponding is increased.

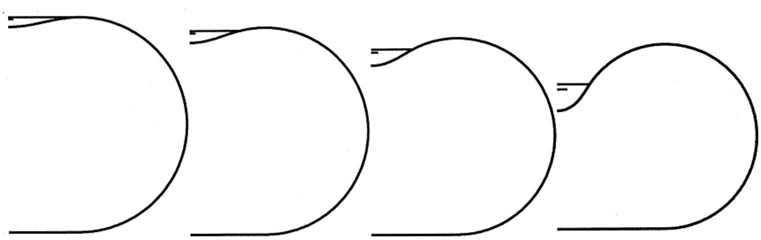

FIG. 2. Typical cross sections for increased ponding on a tube with constant pressure. From left: $\beta = 0.5$, 0.4, 0.3, 0.2.

**Table 2. A typical case for which pressure is maintained constant.**

| $\beta$ | 0.5 | 0.4 | 0.3 | 0.2 |
|---|---|---|---|---|
| $l$ | 50 | 40 | 30 | 20 |
| $\alpha$ | 5.62 | 3.48 | 1.82 | 0.697 |
| $s^*$ | 7.38 | 4.33 | 2.77 | 1.64 |
| $\theta^*$ | 0 | 0.240 | 0.473 | 0.965 |
| $x^*$ | 7.31 | 4.19 | 2.55 | 1.20 |
| $v$ | 3.69 | 2.38 | 1.59 | 0.812 |
| $\hat{x}$ | 7.30 | 6.26 | 5.31 | 4.06 |
| $\hat{y}$ | −21.5 | −16.1 | −10.5 | −4.47 |
| $\hat{s}$ | 42.7 | 33.8 | 24.7 | 15.9 |
| $v/l^2$ | 0.00148 | 0.00149 | 0.00177 | 0.00203 |

Figure 3 shows some typical cross sections for the membrane trough. They depict the membrane deformations as the fluid level gradually rises. In these cases $\alpha$ is always 0.25.

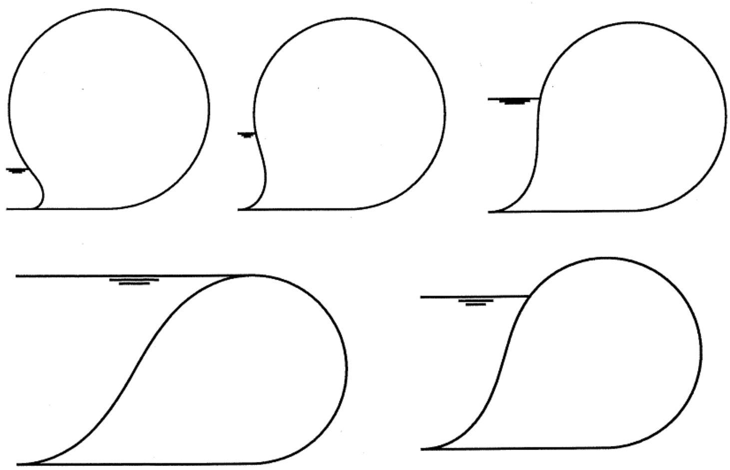

Fig. 3. Cross-sectional shapes for the membrane trough. Clockwise from top: $\beta = 0.1$, 0.2, 0.3, 0.4, 0.5.

Maaskant and Roorda [6] considered the ponding of a membrane arc strip anchored at the two longitudinal edges. Two kinds of instability were found: snap through for shallow arcs and side sway for deep arcs. The membrane tube studied here is never shallow, and snap through phenomenon was not detected. Also, the membrane tube adjusts to any lateral movement of the ponding, therefore it is neutrally stable to side sway.

## 7. Conclusions

Our second-order perturbation solutions, in their range of validity, compare well with those of the exact numerical integration, and thus ascertain both methods.

In comparison to membrane strips which require anchoring and sealing, membrane tubes have the advantage of minimal leakage, easier to transport, set up, and dismantle. This paper considers the ponding of a membrane tube for the first time.

Ponding is usually undesirable. However, the proposed novel membrane trough utilizes ponding as a means of water containment. In addition to the above-mentioned advantages, the membrane trough is automatically anchored.

It is hoped that this paper would elicit further research in these interesting topics.

## References


1. R.N. Dent, *Principles of Pneumatic Architecture*, Wiley, New York, 1972.
2. V. Firt, *Statics, Form-finding, and Dynamics of Air-supported Membrane Structures*, Nijhoft, Hague, 1983.
3. H. Bufler, H. Schneider, *Large strain analysis of rubber-like membranes under dead weight, gas pressure, and hydrostatic loading*, Computational Mechanics, **14**, 165–188, 1994.
4. E. Ghavanloo, F. Daneshmand, *The equilibrium shapes of air-filled heavy membrane tubes resting on inclined planes*, Mechanics Research Communications, **36**, 405–412, 2009.
5. C.Y. Wang, *Load capacity of tethered floating membrane cylinder*, Journal of Engineering Mechanics, **147**, 4, 04021008, 2021.
6. D.J. Malcolm, P.G. Glockner, *Collapse by ponding of air-supported membranes*, ASCE Journal of the Structural Division, **104**, 9, 1525–1532, 1978.
7. S. Lukasiewicz, P.G. Glockner, *Ponding instability of cylindrical air-supported membranes under nonsymmetrical loadings*, Journal of Structural Mechanics, **10**, 4, 419–435, 1983.
8. R. Maaskant, J. Roorda, *Ponding behavior of cylindrical air-supported structures*, Solid Mechanics Archives, **11**, 1, 47–62, 1986.
9. H.O. Anwar, *Inflatable dams*, Proceedings of the American Society of Civil Engineering, **93**-HY3, 99–119, 1967.
10. R. Watson, *A note on the shapes of flexible dams*, Journal of Hydraulic Research, **23**, 2, 179–194, 1985.
11. J.C. Hsieh, R.H. Plaut, *Free vibrations of inflatable dams*, Acta Mechanica, **85**, 207–220, 1990.

12. M. Kim, M. Freeman, B.T. Fitzpatrick, D.B. Nevius, R.H. Plaut, *Use of an apron to stabilize geomembrane tubes for fighting floods*, Geotextiles and Geomembranes, **22**, 239–254, 2004.

*Received February 13, 2021.*
*Published online June 30, 2021.*